A prediction for bubbling geometries

Takuya Okuda

Kavli Institute for Theoretical Physics, University of California,
Santa Barbara, CA 93106, U.S.A.
E-mail: `takuya@kitp.ucsb.edu`

ABSTRACT: We study the supersymmetric circular Wilson loops in $\mathcal{N} = 4$ Yang-Mills theory. Their vacuum expectation values are computed in the parameter region that admits smooth bubbling geometry duals. The results are a prediction for the supergravity action evaluated on the bubbling geometries for Wilson loops.

Contents

1. Introduction and summary

In a holographic correspondence, a quantum gravitational system is exactly equivalent to a non-gravitational theory on a lower dimensional space. In known examples [1, 2] the non-gravitational systems are gauge theories. Gauge invariant observables are mapped to non-normalizable deformations of the gravitational background.

Following progress in understanding the gravity duals of local operators in a gauge theory, the recent years have seen further extension of the dictionary to the realm of non-local gauge invariant operators. The picture that has emerged is strikingly universal for all local and non-local operators. Consider operators of the form $\mathrm{Tr}_R(\ldots)$, where the trace is evaluated in a representation R of $\mathrm{SU}(N)$. We will often use the symbol R to denote the associated Young diagram as well. For different representations R, the operators are best described by different objects on the gravity side. The fundamental representation $R = \square$ corresponds to a fundamental string. A high-rank symmetric representation corresponds to a D-brane, while an anti-symmetric representation is given by another type of D-brane. Finally, an operator with a large rectangular Young diagram is dual to a smooth bubbling geometry with a flux supported on a new cycle. A general Young diagram corresponds to a combination of these objects. This pattern, summarized in figure 1, has been demonstrated for local operators [3 – 7] and Wilson loops [8 – 17] in $\mathcal{N} = 4$ Yang-Mills, as well as for Wilson loops in Chern-Simons theory [2, 18 – 20]. Higher dimensional non-local operators [16, 21 – 25] in gauge theories have descriptions in terms of branes and bubbling geometries.

The identification of the operators and their dual bubbling geometries has been made on the basis of symmetries and charges. An interesting test of the identification, and AdS/CFT itself, would be to compare the expectation value of an operator with the on-shell supergravity action evaluated on the bubbling geometry. For most operators, however,
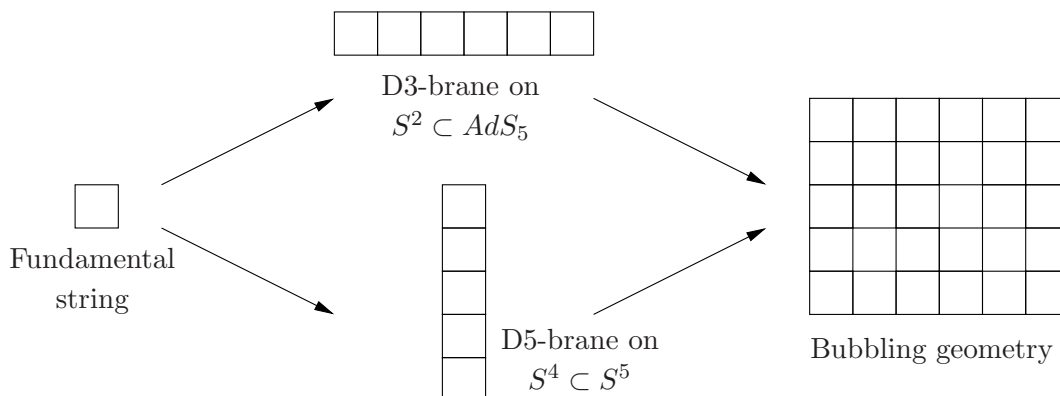
Figure 1: Gravity duals of Wilson loops in $\mathcal{N} = 4$ Yang-Mills. A string corresponds to the fundamental representation, a D3-brane to a symmetric representation, a D5-brane to an anti-symmetric representation, and a bubbling geometry to the representation specified by a rectangular Young diagram. (D3-brane ..., D5-brane ...) in the figure should be replaced by (D3-brane wrapping $S^3 \subset AdS_5$, D3-brane wrapping $S^3 \subset S^5$) for local operators in $\mathcal{N} = 4$ Yang-Mills, and by (D-brane, anti-D-brane) for Wilson loops in Chern-Simons theory.

the test is trivial. the expectation value vanishes for local operators, and does not depend on the coupling for the straight Wilson line. Even if the expectation value does not vanish, the computation in the gauge theory is usually done only in weak coupling. It is then hard to make comparison with the strong coupling computation performed on the gravity side.

In this paper we make a non-trivial prediction for the bubbling geometries dual to particular Wilson loops in $\mathcal{N} = 4$ Yang-Mills, by computing the vevs of the operators on the gauge theory side *in the strong coupling regime*. The operators are the circular supersymmetric Wilson loops defined as

$$W_R \equiv \mathrm{Tr}_R P \exp \oint \left(A + \theta^i \Phi^i ds \right). \tag{1.1}$$

Here $A = A_\mu dx^\mu$ is the gauge field, Φ^i ($i = 1, \ldots, 6$) are the real scalars, s is a parameter for a circle in Euclidean R^4 such that $||dx/ds|| = 1$, and (θ^i) is a constant unit vector in R^6. A smooth bubbling geometry is expected to be dual to a circular Wilson loop whose Young diagram has long edges. More precisely, if we parametrize the diagram as in figure 2, n_I for $I = 1, \ldots, g+1$ and k_I for $I = 1, \ldots, g$ all have to be of order N for the geometry to be smooth. The circular Wilson loop is very special in that such strong coupling computation from gauge theory is possible, due to the conjecture [26] that the Gaussian matrix model captures the circular Wilson loops to all orders in $1/N$ and the 't Hooft coupling $\lambda = g_{\mathrm{YM}}^2 N$.

Relegating the computations to later sections, let us simply summarize the main result: in the limit $N \to \infty$ with n_I/N and k_I/N kept finite, and for the large finite 't Hooft coupling λ, the vev of the circular Wilson loop in the Yang-Mills with gauge group $\mathrm{SU}(N)$
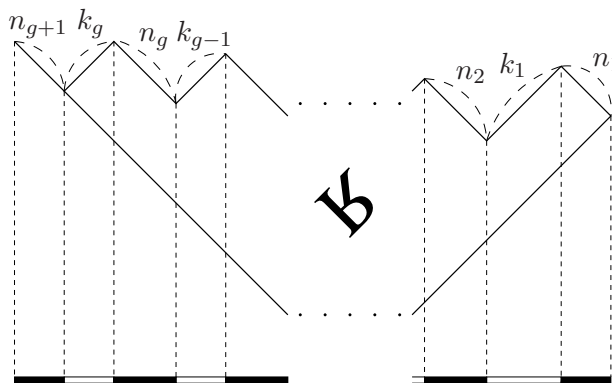
Figure 2: The Young diagram R, shown rotated and inverted, is specified by the lengths n_I and k_I of the edges. Equivalently, n_I and k_I denote the lengths of the black and white regions in the Maya diagram. n_{g+1} is defined by $\sum_{I=1}^{g+1} n_I = N$.

is given by

$$\langle W_R \rangle = \exp\left(\frac{\lambda}{8N} \sum_{I=1}^{g+1} n_I (K_I - |R|/N)^2 + \mathcal{O}(N^2 \log \lambda) \right). \tag{1.2}$$

Here $|R|$ is the n-ality, i.e., the number of boxes in R. We have also defined $K_I = k_I + k_{I+1} + \cdots + k_g$ for $1 \leq I \leq g$ and $K_{g+1} = 0$. An important check of the result is that it is invariant under complex conjugation $R \to \overline{R}$ of the representation, or in terms of the parameters, under

$$n_I \to n_{g+2-I}, \quad k_I \to k_{g+1-I}. \tag{1.3}$$

We expect that the Wilson loop vev is related to the on-shell supergravity action S_{sugra} as

$$\langle W_R \rangle \sim e^{-S_{\text{sugra}}}. \tag{1.4}$$

Note that $\langle W_R \rangle = e^{\mathcal{O}(N^2 \lambda)}$ in our regime. The quadratic dependence on N of the exponent is what is expected from the supergravity action $S_{\text{sugra}} = (1/2\kappa^2) \int \sqrt{g} R + \cdots$ with $\kappa^2 \sim g_s^2 \alpha'^4$, to be evaluated on the dual geometry.

This result is obtained by studying the Gaussian matrix model that captures the correlation functions of circular Wilson loops. In fact we turn the Gaussian matrix model with operator insertions into multi-matrix models whose partition functions are the Wilson loop vevs. We perform the saddle point analysis and propose the eigenvalue distributions. Based on this proposal, we are able to calculate the Wilson loop vevs with the result (1.2).

The circular Wilson loops in Euclidean R^4 can also be thought of as operators in the $\mathcal{N} = 4$ Yang-Mills defined on S^4 [26]. The loop is now the equator of S^4, and the $SO(2) \times SO(3)$ subgroup of the $SO(5)$ isometry group is preserved. The $SO(2)$ is part of the preserved subgroup $SU(1,1)$ of the conformal group $SO(1,5)$. The operator (1.1) also preserves an $SO(5)$ subgroup of the $SO(6)$ R-symmetry group. Thus the bubbling geometry duals of the Wilson loops must solve the BPS equations of the type IIB supergravity with

the $EAdS_2 \times S^2 \times S^4$ ansatz. Note that we need to work with Euclidean signatures since the matrix model captures the circular loop in Euclidean R^4 only. The resulting geometries should be the Euclidean continuation of the solutions recently found in [17].

Given the result of the present paper, the challenge is to use the dual geometries to reproduce the prediction (1.2) by computing the on-shell supergravity action [27]. One would need to deal with such subtle issues as volume regularization, counter terms, and ambiguity of the action due to self-duality of the 5-form flux.[1]

Though the analysis of the matrix models for $\mathcal{N} = 4$ Yang-Mills is in principle sufficient, much confidence in the results and the proposed eigenvalue distributions comes from the study of surprisingly analogous matrix models that describe the Wilson loops in Chern-Simons theory [28–30]. For these matrix models, the resolvents and the spectral curves can be computed exactly in the limit $N \to \infty$, with n_I/N and k_I/N kept finite, without the assumption that the 't Hooft coupling is large. The eigenvalue distributions turn out to be qualitatively the same for the $\mathcal{N} = 4$ Yang-Mills and Chern-Simons theory.

The paper is organized as follows. In section 2, we review the correspondence between the circular Wilson loops in $\mathcal{N} = 4$ Yang-Mills and the observables in the Gaussian matrix model. In section 3 we analyze the Wilson loop with a rectangular Young diagram. Section 4 deals with the Wilson loops in general representations that admit smooth dual bubbling geometries.

2. Gaussian matrix model for circular Wilson loops

It is believed [26, 31] that the correlation functions of circular loops in $\mathcal{N} = 4$ Yang-Mills are captured by the Gaussian matrix model. The precise correspondence states in particular that

$$\left\langle \mathrm{Tr}_R P \exp \oint (A + \theta^i X^i ds) \right\rangle_{\mathrm{U}(N)} = \frac{1}{Z} \int dM \exp\left(-\frac{2N}{\lambda} \mathrm{Tr} M^2 \right) \mathrm{Tr}_R e^M. \qquad (2.1)$$

The left-hand side is the normalized expectation value in the Yang-Mills with gauge group $\mathrm{U}(N)$. The right-hand side is normalized by using the partition function Z which is the integral without the insertion of $\mathrm{Tr}_R e^M$. dM is the standard hermitian matrix measure. In the absence of operator insertions, the eigenvalues are distributed according to the Wigner semi-circle law in the large N limit. The eigenvalue density $\rho(m)$, normalized so that $\int \rho(m) dm = 1$, is given by

$$\rho(m) = \frac{2}{\pi\lambda} \sqrt{\lambda - m^2}. \qquad (2.2)$$

We are also interested in the $\mathrm{SU}(N)$ Yang-Mills theory, for which the conjecture in [26] states that

$$\left\langle \mathrm{Tr}_R P \exp \oint (A + \theta^i X^i ds) \right\rangle_{\mathrm{SU}(N)} = \frac{1}{Z} \int dM \exp\left(-\frac{2N}{\lambda} \mathrm{Tr} M^2 \right) \mathrm{Tr}_R e^{M'}. \qquad (2.3)$$

---

[1]The parallel problem of matching the Wilson loop vev and the closed string partition function has been solved for the Chern-Simons/conifold duality to all orders in genus expansion [18]. The matching of the Wilson loop vevs and the dual on-shell D-brane actions has also been demonstrated [10, 12, 13] for $\mathcal{N} = 4$ Yang-Mills.
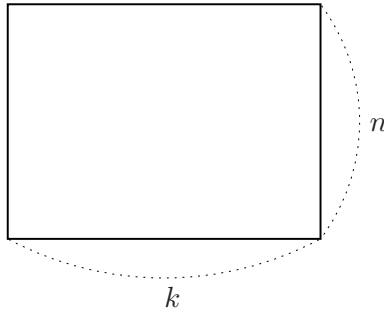
Figure 3: A rectangular Young diagram with n rows and k columns.

Note that on the right-hand side we need the traceless part

$$M' := M - \frac{1}{N}\mathrm{Tr}M \cdot 1_N \qquad (2.4)$$

of the matrix M so that $e^{M'} \in \mathrm{SU}(N)$. The relation

$$\mathrm{Tr}_R e^{M'} = \left(\det e^M\right)^{-|R|/N} \mathrm{Tr}_R e^M \qquad (2.5)$$

will be useful later.

Matrix integrals have been studied intensively in the past, partly motivated by non-critical string theory [32, 33] and relation to supersymmetric gauge theories [34, 35]. In these contexts one does not encounter operators of the form $\mathrm{Tr}_R e^M$ with the Young diagram R that is large both in the row and column directions, and it appears that there is no study of them in the literature.[2]

3. Rectangular Young diagram

In this section, we formulate 2-matrix models whose partition functions are the vev of the Wilson loop with a rectangular Young diagram shown in figure 3. We will have two such matrix models. The first captures the geometric transition of D5-branes wrapping $S^4 \subset S^5$ in $AdS_5 \times S^5$. The second is similarly interpreted in terms of D3-branes wrapping $S^2 \subset AdS_5$. The techniques we introduce here are a generalization of the methods used in [13]. The pictures that emerge are similar to those of [12, 36].

3.1 Eigenvalues as D5-branes

We begin with the Yang-Mills with gauge group $\mathrm{U}(N)$. Let U be a unitary matrix and consider a sum over all the Young diagrams for which the summand is non-vanishing:

$$\sum_R \mathrm{Tr}_R e^M \mathrm{Tr}_{R^T} U = \det\left(1 + e^M \otimes U\right). \qquad (3.1)$$

---

[2]I thank E. Martinec for a discussion on this point.

Here R^T is the transpose of R. This identity, expressed in terms of Schur polynomials as

$$\sum_R s_R(x) s_{R^T}(y) = \prod_{i,j}(1 + x_i y_j) \quad \text{for } x = (x_i) \text{ and } y = (y_j), \tag{3.2}$$

is well-known [37]. The relation can be inverted:

$$\mathrm{Tr}_R e^M = \int dU \det\left(1 + e^M \otimes U^{-1}\right) \mathrm{Tr}_{R^T} U. \tag{3.3}$$

Here dU is the Haar measure on the unitary group normalized so that $\int dU = 1$. We now specialize to the rectangular Young diagram R with n rows and k columns. We choose U to be a $k \times k$ unitary matrix. This choice has a considerable advantage. Let us recall the character formula [38]

$$\mathrm{Tr}_R X = \frac{\det\left(x_b{}^{n-a+R_a}\right)}{\det(x_b{}^{n-a})} \quad \text{for } X = \mathrm{diag}(x_1, \ldots, x_k) \text{ and arbitrary } R, \tag{3.4}$$

where R_a is the number of boxes in the a-th row of R. It implies that

$$\mathrm{Tr}_{R^T} U = (\det U)^n \tag{3.5}$$

for the rectangular diagram R and *for the $k \times k$ matrix U*.[3] By substituting (3.3) and (3.5) into (2.1), we conclude that

$$\langle W_R \rangle_{\mathrm{U}(N)} = \frac{1}{Z} \int dM dU \exp\left(-\frac{2N}{\lambda}\mathrm{Tr}M^2\right) \det(1 + e^M \otimes U^{-1})(\det U)^n. \tag{3.6}$$

By diagonalizing the matrices as

$$M = \mathrm{diag}(m_i)_{i=1}^N, \ U = \mathrm{diag}(e^{u_a})_{a=1}^k, \tag{3.7}$$

and redefining $U \to -U$, the vev can be written as

$$\langle W_R \rangle_{\mathrm{U}(N)} \propto \int \prod_a du_a \prod_i dm_i \exp\left[-\frac{2N}{\lambda}\sum_{i=1}^N m_i^2 + \sum_{i<j}\log(m_i - m_j)^2 + n\sum_{a=1}^k u_a \right. \tag{3.8}$$
$$\left. + \sum_{a<b}\log\left(2\sinh\frac{u_a - u_b}{2}\right)^2 + \sum_{a,i}\log(1 - e^{m_i - u_a}) \right].$$

The constant of proportionality is independent of k and n, is negligible in the precision we work with, and is thus dropped. Since the integrand is analytic, the contours of integration may be deformed. Each u_a is integrated over a period $2\pi i$.

The leading behavior of the Wilson loop vev in the large N limit can be computed in the saddle point approximation. Note that all the terms in the exponent in (3.8) are

---

[3]This can also be understood as follows. A column of length k gives the rank-k anti-symmetric representation A_k. The rectangular diagram R is obtained by symmetrizing n copies of A_k. The representation A_k for $\mathrm{U}(k)$ is one dimensional and the trace in A_k is the determinant. Thus $\mathrm{Tr}_{R^T} U = \mathrm{Tr}_{\mathrm{Sym}^n(A_k)} U = \mathrm{Tr}_{A_k \otimes n} U = (\det U)^n$.

of order N^2. We thus expect a back-reaction of the m-eigenvalue distributions to the u-eigenvalues. This is in contrast to the case with a single row or column [13]. The saddle point equations are

$$-\frac{4N}{\lambda}m_i + 2\sum_{j\neq i}\frac{1}{m_i - m_j} - \sum_a \frac{1}{e^{u_a - m_i} - 1} = 0, \tag{3.9}$$

$$n + \sum_{b\neq a}\coth\frac{u_a - u_b}{2} + \sum_i \frac{1}{e^{u_a - m_i} - 1} = 0. \tag{3.10}$$

One can get useful intuitions by interpreting these equations as force balance conditions. The first term in (3.9) is a restorative force on m_i. The first term in (3.10) represents a constant force applied to each u_a. These are the external forces acting on the system of eigenvalues. The other terms are mutual repulsive forces among m_i's and u_a's.

In the absence of u-eigenvalues, the m-eigenvalues obey Wigner's semicircle law and spread over an interval of width $2\sqrt{\lambda}$. This motivates us to assume that the m- and u-eigenvalues spread over regions of length scale $\sqrt{\lambda}$. Under this assumption that will be justified a posteriori, for large values of λ, we can approximate various expressions as follows:

$$\frac{1}{e^{u_a - m_i} - 1} = \begin{cases} -1 & \text{if } u_a < m_i, \\ 0 & \text{if } m_i < u_a \end{cases}, \tag{3.11}$$

$$\coth\frac{u_a - u_b}{2} = \begin{cases} -1 & \text{if } u_a < u_b, \\ +1 & \text{if } u_b < u_a \end{cases}. \tag{3.12}$$

We now propose an eigenvalue distribution that solves the saddle point equations. Suppose that the eigenvalues m_i split into the first group $\left\{m_i^{(1)} | i = 1, \ldots, n\right\}$ on the right and the second one $\left\{m_i^{(2)} | i = 1, \ldots, N - n\right\}$ on the left. All the u_a's are between them. We also assume that the two groups are far enough from each other so that $1/\left(m_i^{(1)} - m_j^{(2)}\right)$ can be ignored. After we apply (3.11) and (3.12), (3.9) becomes

$$-\frac{4N}{\lambda}m_i^{(1)} + 2\sum_{j\neq i}\frac{1}{m_i^{(1)} - m_j^{(1)}} + k = 0, \tag{3.13}$$

$$-\frac{4N}{\lambda}m_i^{(2)} + 2\sum_{j\neq i}\frac{1}{m_i^{(2)} - m_j^{(2)}} = 0. \tag{3.14}$$

Then the two groups individually obey Wigner's semi-circle law. The first group is spread over an interval of width $2\sqrt{g_s n} = \mathcal{O}\left(\sqrt{\lambda}\right)$ centered at $k\lambda/4N$. For the second group the interval is centered at the origin with width $2\sqrt{g_s(N - n)} = \mathcal{O}\left(\sqrt{\lambda}\right)$. (3.10) simplifies to

$$\sum_{b\neq a}\coth\frac{u_a - u_b}{2} = 0. \tag{3.15}$$

This equation is solved by u_a's uniformly distributed along a line in the imaginary direction. The precise location of the line cannot be determined in this approximation. See figure 4.
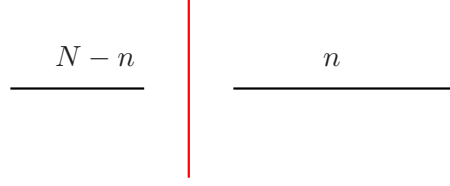
Figure 4: The eigenvalue distributions in the rectangular case. The m-eigenvalues shown as black lines split into two groups, $\{m_i^{(1)}\}$ on the right and $\{m_i^{(2)}\}$ on the left. The u-eigenvalues are distributed uniformly along the red line in the imaginary direction.

The parallel matrix model problem in the Chern-Simons case admits an exact solution for the finite 't Hooft parameter [30]. It exhibits an essentially identical distribution of eigenvalues. This gives us confidence in our proposal of the distribution.

We now use the eigenvalue distribution to evaluate the Wilson loop vev. The exponent in (3.8) can be evaluated, with the help of (3.11) and (3.12), as

$$
-\frac{2N}{\lambda}\sum_i \left(m_i^{(1)}\right)^2 + k\sum_i m_i^{(1)} + \sum_{i<j}\log\left(m_i^{(1)} - m_j^{(1)}\right)^2 - \frac{2N}{\lambda}\sum_i \left(m_i^{(2)}\right)^2 \tag{3.16}
$$

$$
+\sum_{i<j}\log\left(m_i^{(2)} - m_j^{(2)}\right)^2 + \mathcal{O}\left(N^2\log\lambda\right) = \frac{nk^2\lambda}{8N} + \mathcal{O}\left(N^2\log\lambda\right).
$$

The last term arises from completion of squares:

$$
-(2N/\lambda)\left(m_i^{(1)}\right)^2 + km_i^{(1)} = -(2N/\lambda)\left(m_i^{(1)} - k\lambda/4N\right)^2 + k^2\lambda/8N.
$$

We thus conclude that

$$
\langle W_R\rangle_{\mathrm{U}(N)} = \exp\left(\frac{nk^2\lambda}{8N} + \mathcal{O}(N^2\log\lambda)\right). \tag{3.17}
$$

In the $\mathrm{SU}(N)$ case, we need to work with M' defined in (2.4). Because of (2.5), the Wilson loop vev is given by

$$
\langle W_R\rangle_{\mathrm{SU}(N)} = \frac{1}{Z}\int dM\,dU\,e^{-\frac{2N}{\lambda}\mathrm{Tr}M^2}\left(\det e^M\right)^{-\frac{kn}{N}}\det\left(1 + e^M \otimes U^{-1}\right)(\det U)^n. \tag{3.18}
$$

(3.16) is replaced by

$$
-\frac{2N}{\lambda}\sum_i \left(m_i^{(1)}\right)^2 + k\sum_i m_i^{(1)} - \frac{kn}{N}\sum_i m_i^{(1)} + \sum_{i<j}\log\left(m_i^{(1)} - m_j^{(1)}\right)^2
$$

$$
-\frac{2N}{\lambda}\sum_i \left(m_i^{(2)}\right)^2 + \sum_{i<j}\log\left(m_i^{(2)} - m_j^{(2)}\right)^2 - \frac{kn}{N}\sum_i m_i^{(2)}. \tag{3.19}
$$

The leading parts in λ comes from completion of squares:

$$
-\frac{2N}{\lambda}\left(m_i^{(1)}\right)^2 + km_i^{(1)} - \frac{kn}{N}m_i^{(1)} = -\frac{2N}{\lambda}\left(m_i^{(1)} - \frac{\lambda}{4N}k\left(1 - \frac{n}{N}\right)\right)^2 + \frac{\lambda k^2}{8N}\left(1 - \frac{n}{N}\right)^2,
$$

$$
-\frac{2N}{\lambda}\left(m_i^{(1)}\right)^2 - \frac{kn}{N}m_i^{(1)} = -\frac{2N}{\lambda}\left(m_i^{(1)} + \frac{\lambda}{4N}k\frac{n}{N}\right)^2 + \frac{\lambda k^2}{8N}\left(\frac{n}{N}\right)^2.
$$

We find that

$$\langle W_R \rangle_{\mathrm{SU}(N)} = \exp\left(n\frac{\lambda k^2}{8N}\left(1 - \frac{n}{N}\right)^2 + (N-n)\frac{\lambda k^2}{8N}\left(\frac{n}{N}\right)^2 + \mathcal{O}(N^2 \log \lambda) \right)$$

$$= \exp\left(\frac{\lambda k^2}{8N^2}n(N-n) + \mathcal{O}(N^2 \log \lambda) \right). \qquad (3.20)$$

This is the special case of (1.2), and is invariant under $R \to \overline{R}$ or $n \to N-n$ as it should be.

Recall that each column in R represents a D5-brane. Since we have as many u-eigenvalues as columns, we identify the eigenvalues with D5-branes. The back-reaction of the m-eigenvalues to the existence of u-eigenvalues then represents the back-reaction of the geometry to the branes, i.e., geometric transition. Without operator insertions, there is a single black region representing $AdS_5 \times S^5$. The hole in the region, which was identified with D5-branes in [14], is created by the repulsion of m_i and u_a in the present formulation. This is the Wilson loop analog of giant graviton branes represented by a hole in the fermion droplet [7]. In the topological and non-critical string literature [39, 40], it is well-known that the insertion of a determinant operator similar to $\det(1 + e^M \otimes U)$ represents non-compact D-branes. In those cases the eigenvalues of U are the moduli of branes. Here there is a difference: the eigenvalues are first integrated over and are fixed only by saddle point equations.

3.2 Eigenvalue bound states as D3-branes

If we make use of the identity [37, 38]

$$\sum_R \mathrm{Tr}_R V \mathrm{Tr}_R e^M = \frac{1}{\det(1 - V \otimes e^M)} \qquad (3.21)$$

instead of (3.1), we have another expression for $\mathrm{Tr}_R e^M$:

$$\mathrm{Tr}_R e^M = \int dV \frac{1}{\det(1 - V^{-1} \otimes e^M)} \mathrm{Tr}_R V. \qquad (3.22)$$

dV is the Haar measure on the unitary group. More precisely, the contours need to be deformed so that the eigenvalues of V are larger than those of e^M in magnitude. We choose V to be an $n \times n$ unitary matrix, so that

$$\mathrm{Tr}_R V = (\det V)^k \qquad (3.23)$$

for the rectangular Young diagram R. We find that the Wilson loop vev is given by another 2-matrix model

$$\langle W_R \rangle_{\mathrm{U}(N)} = \frac{1}{Z} \int dM dV \exp\left(-\frac{2N}{\lambda}\mathrm{Tr}M^2 \right) \frac{1}{\det(1 - V^{-1} \otimes e^M)}(\det V)^k. \qquad (3.24)$$

By diagonalizing the matrices, we get

$$\langle W_R \rangle_{\mathrm{U}(N)} \propto \int \prod_a dv_a \prod_i dm_i \exp\left[-\frac{2N}{\lambda}\sum_{i=1}^N m_i^2 + \sum_{i<j}\log(m_i - m_j)^2 + k\sum_{a=1}^n v_a \right. \qquad (3.25)$$

$$\left. + \sum_{a<b}\log\left(2\sinh\frac{v_a - v_b}{2} \right)^2 - \sum_{a,i}\log(1 - e^{m_i - v_a}) \right].$$

Let us now analyze this model in the limit $N \to \infty$ with $\lambda, n/N$, and k/N finite.

The saddle point equations are

$$-\frac{4N}{\lambda}m_i + 2\sum_{j\neq i}\frac{1}{m_i - m_j} + \sum_a \frac{1}{e^{v_a - m_i} - 1} = 0, \qquad (3.26)$$

and

$$k + \sum_{b\neq a}\coth\frac{v_a - v_b}{2} - \sum_i \frac{1}{e^{v_a - m_i} - 1} = 0. \qquad (3.27)$$

Again these equations can be interpreted as force balance conditions for the eigenvalues. The difference from the previous subsection is that the interaction between m_i and v_a is *attractive*.

Let us study the eigenvalue distribution for finite but large λ. The v-eigenvalues as a whole are pulled to the right by a force of magnitude kn. Unlike in the previous subsection, we cannot apply (3.11) and (3.12) to the terms involving m_i and v_a. If we did, v_a would only be pulled to the right by m_i, and the force balance would not be achieved. This suggests that each v_a must be very close to m_i.

Each v-eigenvalue is pulled to the right by a force of magnitude k. To balance this, we assume that the v-eigenvalue and an m-eigenvalue sit very close to each other. We also assume, as will be justified a posteriori, that this distance is much smaller than all other length scales in the problem. There are n v-eigenvalues and they are paired up with as many m-eigenvalues $m_i^{(1)}$ ($i = 1, \ldots, n$), forming n *bound states*. The bound states are denoted by $(m\text{-}v)_a$, $a = 1, \ldots, n$. If we order the eigenvalues so that $m_1^{(1)} \lesssim v_1 < m_2^{(1)} \lesssim v_2 < \ldots < m_n^{(1)} \lesssim v_n$, v_a is pushed to the right by $v_1, \ldots, v_{a-1}$.[4] It is also pushed to the left by $v_{a+1}, \ldots, v_n$, but these forces are cancelled by the pull of $m_{a+1}^{(1)}, \ldots, m_n^{(1)}$. Thus (3.27) in the approximation (3.12) becomes

$$k + a - \frac{1}{v_a - m_a^{(1)}} + \mathcal{O}\left(N/\sqrt{\lambda}\right) = 0. \qquad (3.28)$$

The size of the a-th bound state is thus $1/(k+a)$.

Assuming that the group of bound states and the group of remaining m-eigenvalues $\{m_i^{(2)} | i = 1, \ldots, N-n\}$ are far enough from each other, we can replace (3.26) by (3.13) and (3.14). Since the m-eigenvalues are governed by the same equations as in the previous subsection, their distribution is the same. The distribution of the v-eigenvalues is identical to the distribution of $m_i^{(1)}$ on the macroscopic scale. This then justifies the assumptions made in the argument. The computation of the Wilson loop vev is also identical.

Each row in the Young diagram represents a D3-brane [11, 15]. The rectangular diagram R then corresponds to n D3-branes. Since we have the same number of bound states, it is natural to identify each bound state with a D3-brane. This is the analog of an extra droplet in [7] where it was interpreted as dual giant graviton branes wrapping S^3 in AdS_5 .

_____

[4]Strictly speaking, for b such that $0 < a - b \lesssim N/\sqrt{\lambda}$ (3.12) cannot be applied. The error from ignoring the effects, however, is cancelled by the error from ignoring the forces from v_b with $0 < b - a \lesssim N/\sqrt{\lambda}$.
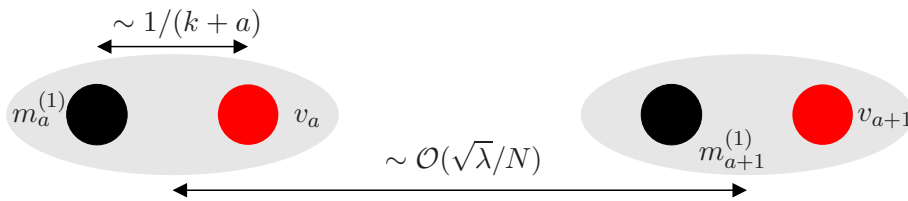
Figure 5: The eigenvalue bound states $(m\text{-}v)_a$. The distance between the two eigenvalues in the a-th bound state from the left is $1/(k+a)$. The distance between neighboring bound states is much larger and is of the order $\sqrt{\lambda}/N$.

Figure 6: The eigenvalue distributions for $M = \text{diag}(m_i)_{i=1}^N$ and $V = \text{diag}(e^{v_a})_{a=1}^n$. $\{m_i\}$ split into two groups $\{m_i^{(1)}\}$ and $\{m_i^{(2)}\}$. The n v_a's are paired with as many $m_i^{(1)}$'s to form n bound states $(m\text{-}v)_a$. These bound states are distributed according to Wigner's semicircle law, as represented by the coincident black and red lines on the right. The distribution of the remaining $N - n$ $m_i^{(2)}$'s independently obeys the semicircle law and is shown on the left.
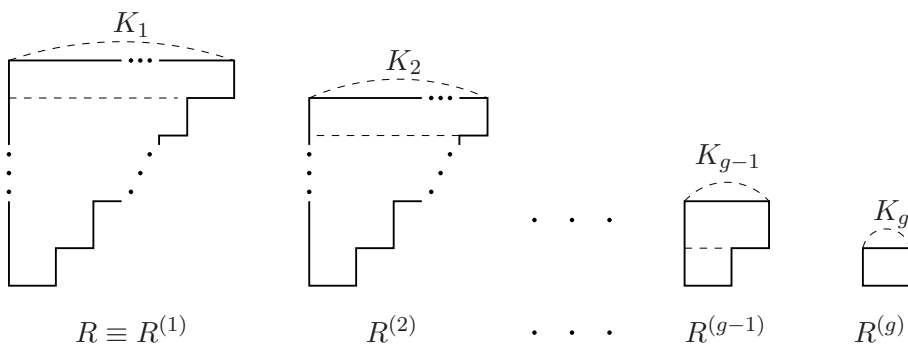

Figure 7: A shrinking sequence of Young diagrams $R \equiv R^{(1)} \supset R^{(2)} \supset \ldots \supset R^{(g)}$.

4. General Young diagram

This section deals with a general Young diagram of the form shown in figure 2, with edge lengths n_I and k_I all of order N. We will obtain two multi-matrix models whose partition functions are the Wilson loop vev.

4.1 Eigenvalue bound states as D5-branes

Let us first see how to generalize the trick that led to 2-matrix models in the rectangle case. We begin with the expression

$$\text{Tr}_R e^M = \int dU^{(1)} \det \left(1 + e^M \otimes U^{(1)-1}\right) \text{Tr}_{R^T} U_1. \tag{4.1}$$

Here $U^{(1)} \in \mathrm{U}(K_1)$. Recall that $K_I \equiv \sum_{J=I}^{g} k_J$. (3.4) in this case allows us to write

$$\mathrm{Tr}_{R^T} U^{(1)} = \left(\det U^{(1)} \right)^{n_1} \mathrm{Tr}_{R^{(2)T}} U^{(1)}. \tag{4.2}$$

Here $R^{(2)}$ is obtained by removing the first n_1 rows from R. See figure 7. Similarly,

$$\mathrm{Tr}_{R^{(2)T}} U^{(1)} = \int dU^{(2)} \frac{1}{\det(1 - U^{(1)} \otimes U^{(2)-1})} \mathrm{Tr}_{R^{(2)T}} U^{(2)}, \tag{4.3}$$

with $U^{(2)}$ in $\mathrm{U}(K_2)$. To be more precise, to avoid singularities the integral is performed along the contours such that the eigenvalues of $U^{(2)}$ are larger than those of $U^{(1)}$ in magnitude. This time we have the relation

$$\mathrm{Tr}_{R^{(2)T}} U^{(2)} = \left(\det U^{(2)} \right)^{n_2} \mathrm{Tr}_{R^{(3)T}} U^{(2)}. \tag{4.4}$$

By removing the first n_2 rows from $R^{(2)}$ one obtains $R^{(3)}$. We now repeat the procedure as many times as we can. This yields

$$
\begin{aligned}
&\mathrm{Tr}_R e^M \\
&= \int dU^{(1)} \det \left(1 + e^M \otimes U^{(1)-1} \right) \left(\det U^{(1)} \right)^{n_1} \int dU^{(2)} \frac{1}{\det(1 - U^{(1)} \otimes U^{(2)-1})} \left(\det U^{(2)} \right)^{n_2} \\
&\quad \ldots \int dU^{(g)} \frac{1}{\det(1 - U^{(g-1)} \otimes U^{(g)-1})} \left(\det U^{(g)} \right)^{n_g}.
\end{aligned} \tag{4.5}
$$

Here $U^{(I)} \in \mathrm{U}(K_I)$, and the integration contours are deformed so that the eigenvalues of $U^{(I)}$ have larger absolute values than those of $U^{(I-1)}$.

We thus have

$$
\begin{aligned}
\langle W_R \rangle_{\mathrm{U}(N)} = &\frac{1}{Z} \int dM dU^{(1)} dU^{(2)} \ldots dU^{(g)} e^{-\frac{2N}{\lambda} \mathrm{Tr} M^2} \left(\det U^{(1)} \right)^{n_1} \left(\det U^{(2)} \right)^{n_2} \ldots \left(\det U^{(g)} \right)^{n_g} \\
&\times \det \left(1 + e^M \otimes U^{(1)-1} \right) \frac{1}{\det(1 - U^{(1)} \otimes U^{(2)-1})} \cdots \frac{1}{\det(1 - U^{(g-1)} \otimes U^{(g)-1})}. \tag{4.6}
\end{aligned}
$$

After redefining $U^{(I)} \to -U^{(I)}$ and diagonalizing the matrices as $M = \mathrm{diag}(m_i)_{i=1}^{N}$, $U^{(I)} = \mathrm{diag}(e^{u_a^{(I)}})_{a=1}^{K_I}$, this becomes

$$
\begin{aligned}
\langle W_R \rangle \propto \int \prod dm_i \prod du_a^{(I)} \exp \Bigg[&-\frac{2N}{\lambda} \sum_{i=1}^{N} m_i^2 + \sum_{I=1}^{g} \sum_{a=1}^{K_I} n_I u_a^{(I)} \\
&+ \sum_{i<j} \log(m_i - m_j)^2 + \sum_I \sum_{a<b} \log \left(2 \sinh \frac{u_a^{(I)} - u_b^{(I)}}{2} \right)^2 \\
&+ \sum_{i,a} \log \left(1 - e^{m_i - u_a^{(1)}} \right) - \sum_I \sum_{a,b} \log \left(1 - e^{u_a^{(I-1)} - u_b^{(I)}} \right) \Bigg]. \tag{4.7}
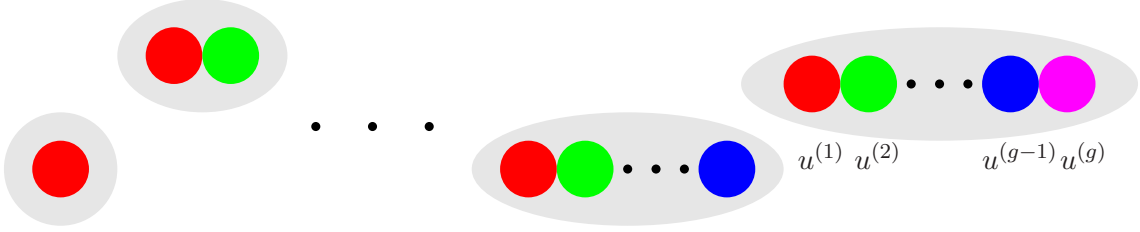\end{aligned}
$$

Figure 8: There are g types of bound states $(u^{(1)}$-$u^{(2)} - \cdots - u^{(I)})$, $I = 1, \ldots, g$.

Our aim is to understand the behavior in the limit $N \to \infty$ with $\lambda, n_I/N, k_I/N$ finite, for large values of λ. The saddle point equations following from the action are

$$-\frac{4N}{\lambda} m_i + \sum_{j \neq i} \frac{2}{m_i - m_j} - \sum_{a=1}^{K_1} \frac{1}{e^{u_a^{(1)} - m_i} - 1} = 0 \text{ for } i = 1, \ldots, N, \quad (4.8)$$

$$n_1 + \sum_{b \neq a} \coth \frac{u_a^{(1)} - u_b^{(1)}}{2} + \sum_{i=1}^{N} \frac{1}{e^{u_a^{(1)} - m_i} - 1} + \sum_{b=1}^{K_2} \frac{1}{e^{u_b^{(2)} - u_a^{(1)}} - 1} = 0$$
$$\text{for } a = 1, \ldots, K_1, \quad (4.9)$$

$$n_I + \sum_{b \neq a} \coth \frac{u_a^{(I)} - u_b^{(I)}}{2} - \sum_{b=1}^{K_{I-1}} \frac{1}{e^{u_a^{(I)} - u_b^{(I-1)}} - 1} + \sum_{b=1}^{K_{I+1}} \frac{1}{e^{u_b^{(I+1)} - u_a^{(I)}} - 1} = 0$$
$$\text{for } I = 2, \ldots, g - 1 \text{ and } a = 1, \ldots, K_I, \quad (4.10)$$

and

$$n_g + \sum_{b \neq a} \coth \frac{u_a^{(g)} - u_b^{(g)}}{2} - \sum_{b=1}^{K_{g-1}} \frac{1}{e^{u_a^{(g)} - u_b^{(g-1)}} - 1} = 0 \text{ for } a = 1, \ldots, K_g. \quad (4.11)$$

All the terms can be interpreted as forces on eigenvalues. Note that the interaction between m_i and $u_a^{(1)}$ is repulsive, while the one between $u_a^{(I)}$ and $u_b^{(I+1)}$ is attractive. This suggests that some eigenvalues form bound states.

Let us work in the $\lambda \to \infty$ approximation. The following distribution of eigenvalues solves the saddle point equations. It involves g types of bound states.[5] The I-th type of bound state, which we denote by $\left(u^{(1)} - u^{(2)} - \cdots - u^{(I)}\right)$, contains a single $u^{(J)}$-eigenvalue for $1 \leq J \leq I$, as shown in figure 8. The m-eigenvalues split into $g + 1$ groups $\{m_i^{(I)} | i = 1, \ldots, n_I\}$. The k_I $(u^{(1)}$-$u^{(2)} - \cdots - u^{(I)})$-bound states are distributed along a line in the imaginary direction, and separate $\{m_i^{(I)}\}$ from $\{m_i^{(I+1)}\}$. See figure 9. For interactions between two bound states or between a bound state and an m-eigenvalue, we can apply (3.11) and (3.12). The $(u^{(1)}$-$u^{(2)} - \cdots - u^{(I)})$-bound state is pulled to the right by an external force of magnitude $n_1 + n_2 + \cdots + n_I$, and pushed back to the left by $n_1 + n_2 + \cdots + n_I$ m-eigenvalues from $\{m_i^{(J)}\}$ for $1 \leq J \leq I$. Bound states of different

---

[5]Though it is convenient to talk about bound states, the size of a bound state is in fact of the same order $\mathcal{O}(1/N)$ as the distance to the neighboring bound state.
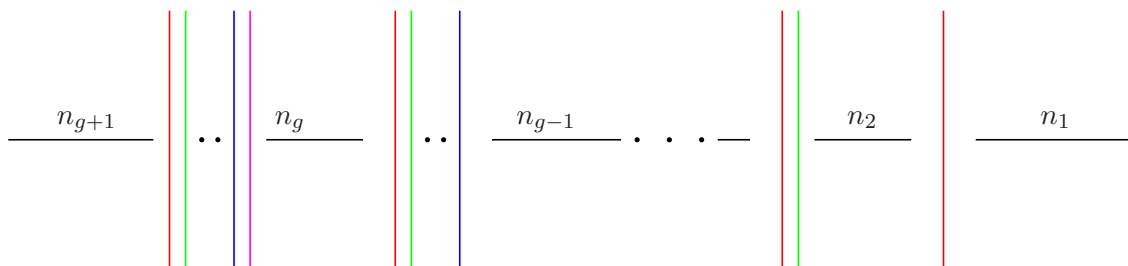
Figure 9: The eigenvalue distributions for M, $U^{(1)}$, $U^{(2)}$,..., $U^{(g-1)}$, and $U^{(g)}$. The N m-eigenvalues split into $g+1$ groups $\{m_i^{(I)}|i=1,\ldots,n_I\}$, $I=1,\ldots,g+1$. The k_I $(u^{(1)}$-$u^{(2)}$-$\cdots$-$u^{(I)})$-bound states are distributed uniformly between $\{m_i^{(I)}\}$ and $\{m_i^{(I+1)}\}$, and are represented by I coincident colored lines in the imaginary direction.

kinds do not interact with each other: forces cancel out among constituent eigenvalues. The saddle point equations are satisfied if the bound states are uniformly distributed along vertical lines. Calculation of relative positions of constituent eigenvalues in a bound state is straightforward. In the bound state $(u^{(1)}$-$u^{(2)}-\cdots-u^{(I)})$, the distance between the $u^{(J)}$- and $u^{(J+1)}$-eigenvalues is $1/(\sum_{K=J+1}^{I} n_K + \sum_{K=J}^{I-1} k_K) = \mathcal{O}(1/N)$ for $1 \leq J \leq I-1$.

It seems reasonable to believe, based on the analogy with [30], that the proposed eigenvalue distribution is the leading saddle point. Let us calculate the Wilson loop vev by using the proposed distribution. The exponent of (4.7) becomes

$$-\frac{2N}{\lambda}\sum_{I=1}^{g+1}\sum_{i=1}^{n_I}\left(m_i^{(I)}\right)^2 + \sum_{I=1}^{g}\sum_{i=1}^{n_I}K_I m_i^{(I)} + \sum_{I=1}^{g+1}\sum_{i<j}\log\left(m_i^{(I)}-m_j^{(I)}\right)^2 + \mathcal{O}(N^2\log\lambda) \quad (4.12)$$

$$= \sum_{I=1}^{g}\frac{\lambda}{8N}n_I K_I^2 + \mathcal{O}(N^2\log\lambda).$$

We get the final result for the U(N) Yang-Mills:

$$\langle W_R\rangle_{\mathrm{U}(N)} = \exp\left(\sum_{I=1}^{g}\frac{\lambda}{8N}n_I K_I^2 + \mathcal{O}(N^2\log\lambda)\right). \quad (4.13)$$

In the SU(N) case, (2.5) allows us to write

$$\langle W_R\rangle_{\mathrm{SU}(N)} = \frac{1}{Z}\int dM\,dU^{(1)}\,dU^{(2)}\ldots dU^{(g)}e^{-\frac{2N}{\lambda}\mathrm{Tr}M^2}\left(\det e^M\right)^{-|R|/N}$$

$$\times\left(\det U^{(1)}\right)^{n_1}\left(\det U^{(2)}\right)^{n_2}\ldots\left(\det U^{(g)}\right)^{n_g}\det\left(1+e^M\otimes U^{(1)-1}\right)$$

$$\times\frac{1}{\det(1-U^{(1)}\otimes U^{(2)-1})}\cdots\frac{1}{\det(1-U^{(g-1)}\otimes U^{(g)-1})}. \quad (4.14)$$
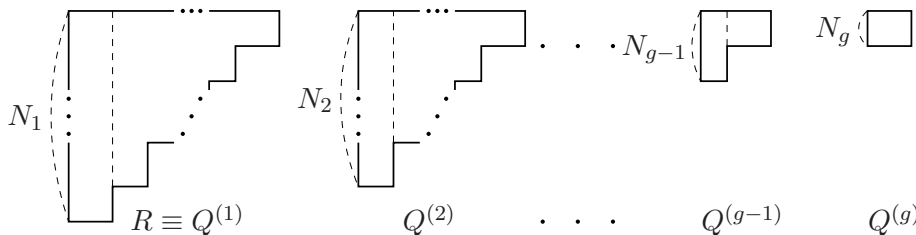
Figure 10: Another shrinking sequence of Young diagrams $R \equiv Q^{(1)} \supset Q^{(2)} \supset \ldots \supset Q^{(g)}$.

(4.12) is replaced by

$$-\frac{2N}{\lambda}\sum_{I=1}^{g+1}\sum_i \left(m_i^{(I)}\right)^2 + \sum_{I=1}^{g+1}\sum_i \left(K_I - |R|/N\right)m_i^{(I)} \tag{4.15}$$
$$+ \sum_{I=1}^{g+1}\sum_{i<j}\log\left(m_i^{(I)}-m_j^{(I)}\right)^2 + \mathcal{O}\left(N^2\log\lambda\right)$$
$$= \sum_{I=1}^{g+1}\frac{\lambda}{8N}n_I(K_I-|R|/N)^2 + \mathcal{O}(N^2\log\lambda).$$

Recall that $K_{g+1}\equiv 0$. This is the result (1.2) presented in the introduction.

4.2 Eigenvalue bound states as D3-branes

Another matrix model can be obtained by starting with the formula

$$\mathrm{Tr}_R e^M = \int dV^{(1)} \frac{1}{\det(1-e^M\otimes V^{(1)-1})}\mathrm{Tr}_R V^{(1)}. \tag{4.16}$$

Here $V^{(1)}\in \mathrm{U}(N_1)$ and $dV^{(1)}$ is the Haar measure. We have defined $N_I := \sum_{J=1}^{g+1-I} n_J$. Note that

$$\mathrm{Tr}_R V^{(1)} = \left(\det V^{(1)}\right)^{k_g}\mathrm{Tr}_{Q^{(2)}}V^{(1)}. \tag{4.17}$$

Here $Q^{(2)}$ is obtained by removing the first k_g rows from R. See figure 10. Similarly,

$$\mathrm{Tr}_{Q^{(2)}}V^{(1)} = \int dV^{(2)}\frac{1}{\det(1-V^{(1)}\otimes V^{(2)-1})}\mathrm{Tr}_{Q^{(2)}}V^{(2)}, \tag{4.18}$$

with $V^{(2)}$ essentially in $\mathrm{U}(N_2)$. To avoid singularities the integral is performed along appropriate contours. We repeat the same procedure as many times as possible. This gives

$$\mathrm{Tr}_R e^M = \int dV^{(1)}\frac{1}{\det(1-e^M\otimes V^{(1)-1})}(\det V^{(1)})^{k_g}\int dV^{(2)}\frac{1}{\det(1-V^{(1)}\otimes V^{(2)-1})}$$
$$\times \left(\det V^{(2)}\right)^{k_{g-1}}\ldots\int dV^{(g)}\frac{1}{\det(1-V^{(g-1)}\otimes V^{(g)-1})}\left(\det V^{(g)}\right)^{k_1}. \tag{4.19}$$

Here $V^{(I)}\in \mathrm{U}(N_I)$, and the integration contours are deformed so that the eigenvalues of $V^{(I)}$ have larger absolute values than $V^{(I-1)}$.

We thus have

$$\langle W_R \rangle = \frac{1}{Z} \int dM \, dV^{(1)} dV^{(2)} \ldots dV^{(g)} e^{-\frac{2N}{\lambda} \mathrm{Tr} M^2} \left(\det V^{(1)} \right)^{k_g} \left(\det V^{(2)} \right)^{k_{g-1}} \ldots \left(\det V^{(g)} \right)^{k_1}$$

$$\times \frac{1}{\det(1 - e^M \otimes V^{(1)-1})} \frac{1}{\det(1 - V^{(1)} \otimes V^{(2)-1})} \cdots \frac{1}{\det(1 - V^{(g-1)} \otimes V^{(g)-1})}. \quad (4.20)$$

In terms of the eigenvalues, the Wilson loop is given by

$$\langle W_R \rangle \propto \int \prod dm_i \prod dv_a^{(I)} \exp \left[-\frac{2N}{\lambda} \sum_{i=1}^N m_i^2 + \sum_{I=1}^g \sum_{a=1}^{N_I} k_{g+1-I} v_a^{(I)} \right. \quad (4.21)$$

$$+ \sum_{i<j} \log(m_i - m_j)^2 + \sum_I \sum_{a<b} \log \left(2 \sinh \frac{v_a^{(I)} - v_b^{(I)}}{2} \right)^2$$

$$\left. - \sum_{i,a} \log \left(1 - e^{m_i - v_a^{(1)}} \right) - \sum_I \sum_{a,b} \log \left(1 - e^{v_a^{(I-1)} - v_b^{(I)}} \right) \right].$$

Let us study this model in the large N limit with n_I/N and k_I/N fixed. The saddle point equations are

$$-\frac{4N}{\lambda} m_i + \sum_{j \neq i} \frac{2}{m_i - m_j} + \sum_{a=1}^{N_1} \frac{1}{e^{v_a^{(1)} - m_i} - 1} = 0 \text{ for } i = 1, \ldots, N,$$

$$(4.22)$$

$$k_g + \sum_{b \neq a} \coth \frac{v_a^{(1)} - v_b^{(1)}}{2} - \sum_{i=1}^N \frac{1}{e^{v_a^{(1)} - m_i} - 1} + \sum_{b=1}^{N_2} \frac{1}{e^{v_b^{(2)} - v_a^{(1)}} - 1} = 0$$

$$\text{for } a = 1, \ldots, N_1, \quad (4.23)$$

$$k_{g+1-I} + \sum_{b \neq a} \coth \frac{v_a^{(I)} - v_b^{(I)}}{2} - \sum_{b=1}^{N_{I-1}} \frac{1}{e^{v_a^{(I)} - v_b^{(I-1)}} - 1} + \sum_{b=1}^{N_{I+1}} \frac{1}{e^{v_b^{(I+1)} - v_a^{(I)}} - 1} = 0$$

$$\text{for } I = 2, \ldots, g-1 \text{ and } a = 1, \ldots, N_I, \quad (4.24)$$

and

$$k_1 + \sum_{b \neq a} \coth \frac{v_a^{(g)} - v_b^{(g)}}{2} - \sum_{b=1}^{N_{g-1}} \frac{1}{e^{v_a^{(g)} - v_b^{(g-1)}} - 1} = 0 \text{ for } a = 1, \ldots, N_g, \quad (4.25)$$

The forces between m_i and $v_a^{(1)}$ as well as between $v_a^{(I)}$ and $v_b^{(I+1)}$ are attractive.

Our proposed distribution of the eigenvalues for large λ is as follows. There are g types of bound states denoted by $(m\text{-}v^{(1)} - \cdots - v^{(I)})$ for $I = 0, 1, \ldots, g$. Each bound state of the I-th type has a single m-eigenvalue as well as a single $v^{(J)}$-eigenvalue for $1 \leq J \leq I$. The size of a bound state is of the order $1/N$, and is much smaller than the distance between two neighboring bound states. The n_{g+1-I} $(m\text{-}v^{(1)} - \cdots - v^{(I)})$-bound states are distributed according to the semi-circle law centered at $\lambda k_I/4N$. Using (3.11) and (3.12), one can confirm that the force balance among bound states is achieved. It is
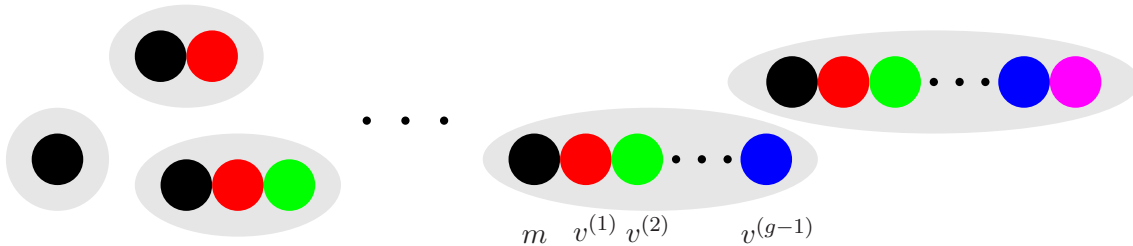
Figure 11: $g + 1$ types of bound states $(m\text{-}v^{(1)} - \cdots - v^{(I)})$, $I = 0, 1, \ldots, g$.
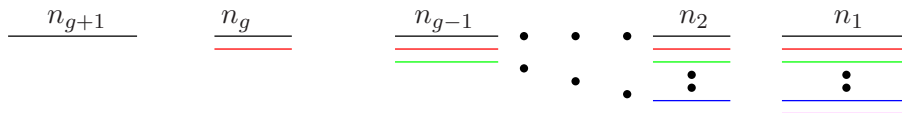

Figure 12: The eigenvalue distributions for M, $V^{(1)}$, $V^{(2)}$,..., $V^{(g-1)}$, $V^{(g)}$. The n_{g+1-I} $(m\text{-}v^{(1)} - \cdots - v^{(I)})$-bound states are distributed according to Wigner's semi-circle law.

straightforward to calculate the distance between eigenvalues in a bound state. In the a-th $(m\text{-}v^{(1)} - \cdots - v^{(I)})$ bound state, the distance between the $v^{(J)}$- and $v^{(J+1)}$-eigenvalues turns out to be $1/((I - J)a + \sum_{K=J}^{I} k_{g+1-K}) = \mathcal{O}(1/N)$ for $0 \leq J \leq I - 1$. Here $v^{(0)} \equiv m$ and $k_{g+1} \equiv 0$. This configuration solves the saddle point equations. The distribution of the m-eigenvalues is identical to the one in the previous subsection, and leads to the same results for the Wilson loop vev.

Acknowledgments

References

[1] J.M. Maldacena, *The large-N limit of superconformal field theories and supergravity*, Adv. Theor. Math. Phys. **2** (1998) 231 [*Int. J. Theor. Phys.* **38** (1999) 1113] [`hep-th/9711200`].

[2] R. Gopakumar and C. Vafa, *On the gauge theory/geometry correspondence*, Adv. Theor. Math. Phys. **3** (1999) 1415 [`hep-th/9811131`].

[3] J. McGreevy, L. Susskind and N. Toumbas, *Invasion of the giant gravitons from anti-de Sitter space*, JHEP **06** (2000) 008 [`hep-th/0003075`].

[4] A. Hashimoto, S. Hirano and N. Itzhaki, *Large branes in AdS and their field theory dual*, JHEP **08** (2000) 051 [`hep-th/0008016`].

[5] V. Balasubramanian, M. Berkooz, A. Naqvi and M.J. Strassler, *Giant gravitons in conformal field theory*, JHEP **04** (2002) 034 [`hep-th/0107119`].

[6] S. Corley, A. Jevicki and S. Ramgoolam, *Exact correlators of giant gravitons from dual N = 4 SYM theory*, *Adv. Theor. Math. Phys.* **5** (2002) 809 [hep-th/0111222].

[7] H. Lin, O. Lunin and J.M. Maldacena, *Bubbling AdS space and 1/2 BPS geometries*, *JHEP* **10** (2004) 025 [hep-th/0409174].

[8] J.M. Maldacena, *Wilson loops in large-N field theories*, *Phys. Rev. Lett.* **80** (1998) 4859 [hep-th/9803002].

[9] S.-J. Rey and J.-T. Yee, *Macroscopic strings as heavy quarks in large-N gauge theory and anti-de Sitter supergravity*, *Eur. Phys. J.* **C 22** (2001) 379 [hep-th/9803001].

[10] N. Drukker and B. Fiol, *All-genus calculation of Wilson loops using D-branes*, *JHEP* **02** (2005) 010 [hep-th/0501109].

[11] J. Gomis and F. Passerini, *Holographic Wilson loops*, *JHEP* **08** (2006) 074 [hep-th/0604007].

[12] S. Yamaguchi, *Wilson loops of anti-symmetric representation and D5-branes*, *JHEP* **05** (2006) 037 [hep-th/0603208].

[13] S.A. Hartnoll and S.P. Kumar, *Higher rank Wilson loops from a matrix model*, *JHEP* **08** (2006) 026 [hep-th/0605027].

[14] S. Yamaguchi, *Bubbling geometries for half BPS Wilson lines*, *Int. J. Mod. Phys.* **A 22** (2007) 1353 [hep-th/0601089].

[15] J. Gomis and F. Passerini, *Wilson loops as D3-branes*, *JHEP* **01** (2007) 097 [hep-th/0612022].

[16] O. Lunin, *On gravitational description of Wilson lines*, *JHEP* **06** (2006) 026 [hep-th/0604133].

[17] E. D'Hoker, J. Estes and M. Gutperle, *Gravity duals of half-BPS Wilson loops*, *JHEP* **06** (2007) 063 [arXiv:0705.1004].

[18] J. Gomis and T. Okuda, *Wilson loops, geometric transitions and bubbling Calabi-Yau's*, *JHEP* **02** (2007) 083 [hep-th/0612190].

[19] J. Gomis and T. Okuda, *D-branes as a bubbling Calabi-Yau*, *JHEP* **07** (2007) 005 [arXiv:0704.3080].

[20] T. Okuda, *Bions in topological string theory*, arXiv:0705.0722.

[21] S. Gukov and E. Witten, *Gauge theory, ramification and the geometric Langlands program*, hep-th/0612073.

[22] J. Gomis and S. Matsuura, *Bubbling surface operators and S-duality*, *JHEP* **06** (2007) 025 [arXiv:0704.1657].

[23] A. Karch and L. Randall, *Open and closed string interpretation of SUSY CFT's on branes with boundaries*, *JHEP* **06** (2001) 063 [hep-th/0105132].

[24] J. Gomis and C. Romelsberger, *Bubbling defect CFT's*, *JHEP* **08** (2006) 050 [hep-th/0604155].

[25] O. Lunin, *1/2-BPS states in M-theory and defects in the dual CFTs*, *JHEP* **10** (2007) 014 [arXiv:0704.3442].

[26] N. Drukker and D.J. Gross, *An exact prediction of N = 4 SUSYM theory for string theory*, *J. Math. Phys.* **42** (2001) 2896 [hep-th/0010274].

[27] T. Okuda and D. Trancanelli, *work in progress*.

[28] M. Mariño, *Chern-Simons theory, matrix integrals and perturbative three-manifold invariants*, *Commun. Math. Phys.* **253** (2004) 25 [`hep-th/0207096`].

[29] M. Aganagic, A. Klemm, M. Mariño and C. Vafa, *Matrix model as a mirror of Chern-Simons theory*, *JHEP* **02** (2004) 010 [`hep-th/0211098`].

[30] N. Halmagyi and T. Okuda, *Bubbling Calabi-Yau's from matrix models*, to appear.

[31] J.K. Erickson, G.W. Semenoff and K. Zarembo, *Wilson loops in $N = 4$ supersymmetric Yang-Mills theory*, *Nucl. Phys.* **B 582** (2000) 155 [`hep-th/0003055`].

[32] P.H. Ginsparg and G.W. Moore, *Lectures on 2D gravity and 2D string theory*, `hep-th/9304011`.

[33] P. Di Francesco, P.H. Ginsparg and J. Zinn-Justin, *2D gravity and random matrices*, *Phys. Rept.* **254** (1995) 1 [`hep-th/9306153`].

[34] R. Dijkgraaf and C. Vafa, *Matrix models, topological strings and supersymmetric gauge theories*, *Nucl. Phys.* **B 644** (2002) 3 [`hep-th/0206255`].

[35] R. Dijkgraaf and C. Vafa, *A perturbative window into non-perturbative physics*, `hep-th/0208048`.

[36] S. Yamaguchi, *Semi-classical open string corrections and symmetric Wilson loops*, *JHEP* **06** (2007) 073 [`hep-th/0701052`].

[37] I. Macdonald, *Symmetric functions and Hall polynomials*, second edition, Oxford university press, Oxford U.K. (1995).

[38] J. Fulton and W. Harris, *Representation theory: a first course*, Graduate Texts in Mathematics, Springer-Verlag (1999).

[39] M. Aganagic, R. Dijkgraaf, A. Klemm, M. Mariño and C. Vafa, *Topological strings and integrable hierarchies*, *Commun. Math. Phys.* **261** (2006) 451 [`hep-th/0312085`].

[40] J.M. Maldacena, G.W. Moore, N. Seiberg and D. Shih, *Exact vs. semiclassical target space of the minimal string*, *JHEP* **10** (2004) 020 [`hep-th/0408039`].